Silicon (2022) 14:4411–4422
https://doi.org/10.1007/s12633-021-01281-3

ORIGINAL PAPER

Functionalized Nanosilica for Vulcanization Efficiency and Mechanical Properties of Natural Rubber Composites

P. Dileep[1,2] · Sinto Jacob[3] · C. S. Julie Chandra[4] · C. D. Midhun Dominic[5] · M. P. Poornima[6] · John P. Rappai[7] · Sunil K. Narayanankutty[1]

Received: 22 April 2021 / Accepted: 15 July 2021 / Published online: 6 August 2021

Abstract

Accelerator functional character was introduced on nanosilica by chemical reaction of sodium isopropyl xanthate (SIPX) with nanosilica (NS). Functional characteristics of nanosilica were confirmed by elemental analysis, thermogravimetric analysis, and infrared spectroscopy. This SIPX functionalized nanosilica (SIPX-NS) incorporated natural rubber (NR) composites were used to evaluate the dispersion of silica in rubber and also the interaction between rubber and filler. The finely dispersed SIPX-NS particles in the NR matrix are revealed from the morphological analysis. Subtle changes in the surface chemistry of silica had a profound influence on dispersibility in the NR matrix. NR 4SIPX-NS composite showed an increase in tensile strength by 10%, flex crack initiation resistance by 13%, tensile strength retention by 16% and cure time reduced by 2 min relative to those of NR 3NS composite. This simple, efficient and cost-effective surface modification of silica improved the vulcanization efficiency and mechanical performance of NR composites and has great potential in the fabrication of high-performance polymer composites.

Keywords Nanosilica · Surface modification · Sodium isopropyl xanthate · Thermal conductivity · Flex crack resistance

1 Introduction

Nanosilica is an emerging environment-friendly nanofiller used for the reinforcement of elastomers and is not derived from petroleum resources [1, 2]. These nanoparticles have high surface energy and a tendency to agglomerate because of the groups like siloxane and silanol present on silica surfaces [3]. To overcome this disadvantage, modification of its surface chemistry is necessary to improve its dispersion properties and compatibility in an organic matrix.

The surface modification of silica particles can be achieved by different methods such as organoalkoxysilane modification [4, 5], polymer grafting [6, 7], encapsulation [8, 9], etc. The surface modified silica with organosilanes is used in polymer

Highlights - Sodium isopropyl xanthate (SIPX) is an efficient accelerator for silica modification.
- SIPX- bound nanosilica reduces cure time of natural rubber (NR) compounds.
- SIPX modification leads to improved silica - rubber interaction.
- Thermal aging properties of NR composites are improved by SIPX-NS addition.

✉ P. Dileep
pdileep84@gmail.com; dr@rubberparkindia.org

[1] Department of Polymer Science and Rubber Technology, Cochin University of Science and Technology (CUSAT), Cochin 682022, India

[2] J J Murphy Research Centre, Rubber Park India Pvt. Ltd., Airapuram, Kerala 683556, India

[3] Department of Chemistry, St. Aloysius College, Elthuruth, Thrissur, Kerala 680611, India

[4] Department of Chemistry, Maharaja's College, Ernakulam, Kerala 682011, India

[5] Department of Chemistry, Sacred Heart College, Thevara, Kochi, Kerala 682013, India

[6] Department of Chemistry, Sree Sankara Vidyapeetom College, Valayanchirangara, Kochi, Kerala 683556, India

[7] Department of Chemistry, Govt. Victoria College, Palakkad, Kerala 678001, India

and rubber industry for the improving mechanical properties. The surface interface between the polymer and filler surface affects the nonlinear viscoelastic behaviour and improves the mechanical properties as well as energy efficiency of rubber nanocomposites [10]. Zhang et al. found that the addition of a silane coupling agent (Si 69) modified silica reduced the rolling resistance and heat build-up of NR composites [11]. Chen et al. proposed a surface modification of silica with sulphur monochloride by the reaction between silanol hydroxyl groups in silica and chlorine atom in sulphur monochloride [12]. This silica-supported sulphur monochloride improved the cure efficiency and tensile strength of SBR composites. The silica-supported vulcanizing accelerator was prepared by grafting 2-benzothiazolethiol onto the surface of silane modified silica to improve the silica-matrix interaction and silica dispersion in SBR [13]. Mathew et al. found that SBR composites containing plasma treated silica could improve the tensile strength and modulus of SBR composites [14]. Wang et al. developed surface modified silica nanoparticles by combining noncovalent and covalent modification processes in a simple, efficient and cost-effective method [15]. Weng et al. also developed a new protocol to promote the dispersion of silica and interfacial strength along with reduced abrasion loss in SBR/silica composites by grafting with oniums [16]. Liu et al. established a simple inhibition-grafting method to prepare silica/polydimethylsiloxane nanocomposites with superior tensile strength, tear strength and low viscosity [17]. Guo et al. directly blended sorbic acid during SBR/silica compounding and the addition of 15 phr sorbic acid increased the storage modulus and reduced the glass transition temperature due to the deagglomeration of silica particles in SBR matrix [18]. Gill et al. prepared NBR/Chitosan/ nanosilanized silica blends and observed improved crosslink density and hardness upon nano-silanized silica loading [19].

Natural rubber, an unsaturated elastomer has been widely used due to its excellent elastic property. However, low polarity, poor oil resistance and low air impermeability of NR limit its applications in some cases [20]. To overcome these drawbacks, NR is modified appropriately. Xu et al. used epoxidised natural rubber (ENR) as an interfacial modifier to improve the mechanical and dynamical mechanical properties of NR/silica composites [21]. The results indicate the formation of a covalent bond by the ring-opening reaction between the epoxy groups of ENR chains and Si-OH groups on the silica surfaces. Ismail et al. selected maleated natural rubber as a coupling agent for paper sludge fiber filled NR composites and found excellent rheological and dynamic properties [22]. According to Gelling, NR backbone stereo-regularity was disrupted by any type of chemical modifications and hence, reduction in basic strength properties of NR [23].

After a thorough investigation of the literature, we came to know that the surface modification of silica with suitable coupling agents is a classical way to improve the interfacial adhesion between particles of silica and natural rubber. The surface modification not only improves the hydrophilic- hydrophobic interactions between silica and NR but also enhances the dispersion of silica in the NR matrix. Even though the silane modification has several advantages, the high cost of silane coupling agents and the high processing temperature required for the efficient surface modification limit its applications. So, the surface modification of silica with a cost-effective and efficient surface modifier with unique properties is a need of the hour. Herein, we report the use of sodium isopropyl xanthate (SIPX) as a novel surface modifier for silica. To our best knowledge, no studies have been reported so far to evaluate the role of SIPX modified silica in NR. Nanosilica with high surface area (520 m2/g) derived from bamboo leaves in the present study is also remarkable. The surface modification and its size distribution were characterized by FTIR, TGA, EDX, SEM and dynamic light scattering (DLS). Modification of nanosilica improved curing, mechanical performance, crosslink density and aging resistance of NR.

Table 1 Formulation of NR mixes

Ingredients* (phr)[a]	Mix Names				
	NR Gum	NR 3NS	NR 3SIPX-NS	NR 4SIPX-NS	NR 5SIPX-NS
ISNR-5	100	100	100	100	100
NS	0	3	0	0	0
SIPX-NS	0	0	3	4	5
DEG	0	0.3	0.3	0.4	0.5

*Zinc oxide 5.0, stearic acid 2.0, styrenated phenol 1.0, Tetramethylthiuram disulphide 0.2, N-cyclohexyl-2-benzothiazole sulphenamide 0.6 and sulphur 2.5 were added in all formulations

[a] parts per hundred of rubber

2 Experimental

2.1 Materials

Rubber Research Institute of India (RRII), Kottayam provided ISNR-5 grade Natural Rubber with 70 ± 2 Mooney viscosity (ML 1 + 4 @ 100 °C). Nano-sized silica particles (520 m^2/g surface area) synthesized from bamboo leaves. The detailed procedure for the extraction of silica from bamboo leaves is reported in our previously reported work [24]. Sodium isopropyl xanthate (SIPX) was purchased from Amruta Industries, Mumbai, India. Commercial grade tetramethylthiuram disulphide (TMTD), stearic acid, sulphur (S), N-cyclohexyl-2-benzothiazole sulphenamide (CBS), and zinc oxide (ZnO) were used as received. Toluene and diethylene glycol (DEG)

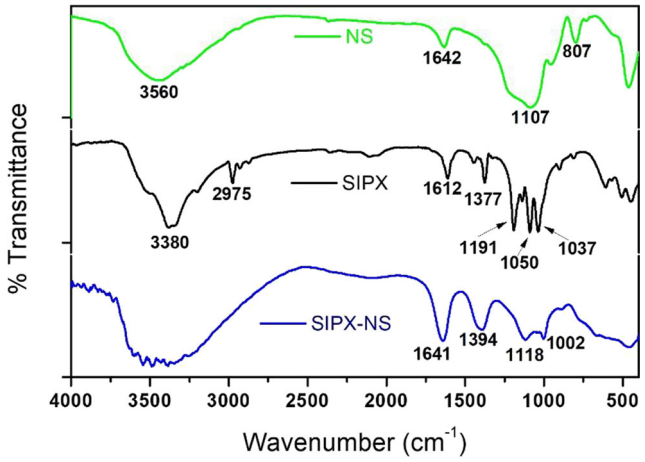

Fig. 1 FTIR spectra of NS, SIPX and SIPX-NS

were purchased from Merck Specialties Private Limited, India.

2.2 Methods

2.2.1 Modification of Nanosilica with Vulcanizing Accelerator SIPX

5 g of SIPX was dissolved in 50 mL of isopropyl alcohol and to this solution, 10 g of nanosilica (dried at 100 °C for 6 h) was added. This mixture was heated at 80 °C for 24 h with continuous stirring. The unreacted SIPX was then removed from the reaction mixture by soxhlet extraction using isopropyl alcohol for about 8 h. The residue obtained was vacuum dried at 50 °C for 3 h to obtain SIPX modified nanosilica (SIPX-NS).

2.2.2 Composites Preparation

Thermo Haake Polylab with a rotor speed of 60 rpm maintained at 70 °C was used for compounding as per ASTM D 3184. Table 1 gives the details of formulation. Initially, mastication of NR was done for 3 min. Stearic acid, zinc oxide and styrenated phenol were then added followed by DEG and nanosilica and the compound was mixed for 3 min. TMTD, CBS and sulphur were added and the mixing was continued for 2 min. After 8 min of mixing, the compound was sheeted out at 5 mm nip gap (5 times) by using a laboratory size (6”×12”) two-roll mill and finally sheeted out the compound at a 3 mm nip gap. Before moulding, this compound was allowed to mature for 24 h at room temperature. A hydraulic press having 12”×12” platen size was used to vulcanize this compound to the optimum cure time at 150 °C temperature and 150 kg/cm^2 pressure.

Table 2 Elemental analysis of SIPX-NS

Materials	Elements (wt%)				
	Si	O	C	Na	S
NS	49.54	50.46	-	-	-
SIPX-NS	38.97	48.95	5.73	4.04	2.31

2.3 Characterization Methods

2.3.1 Fourier Transform Infrared Spectroscopy

Fourier transform infrared analysis was conducted using Thermo Nicolet, Avatar 370 model IR spectrometer, in 4000–400 cm^{-1} spectral range with a resolution of 4 cm^{-1}. Here transmittance (%) is plotted as the function of wavenumber (cm^{-1}).

2.3.2 Energy Dispersive X-Ray Spectroscopy

JEOL (JED-2300 Model) instrument was used to perform EDX (Energy Dispersive X-ray) analysis. Malvern mastersizer-V3.30 instrument capable of measuring size between 0.1 to 1000 μm and an angular range of 0.032–60 degrees was used to measure the particle size distribution.

2.3.3 Dynamic Light Scattering

The particle size of nanosilica dispersion in water was measured using Horiba scientific nano particle analyzer SZ-100 with a scattering angle of 173 degrees.

2.3.4 Scanning Electron Microscope

The scanning electron microscope of JOEL (Model JSM 8390 LV) was used to analyze the tensile fractured surfaces. Sample surfaces were sputtered with a thin layer of gold before the analysis to avoid charging on the surface.

2.3.5 Thermogravimetric Analysis

Thermogravimetric analyser (TA instruments, model Q-50) was used to perform thermogravimetric analysis. Samples were kept in a nitrogen atmosphere and heated from room temperature to 750 °C at a heating rate of 20 °C/min.

2.3.6 Thermal Conductivity

Thermal conductivity was measured according to ASTM D7340 using Holmarc’s Lee’s Disc Apparatus (Model: HOAE-LD18). The apparatus comprises a brass disc resting on another slab of the same dimension with a special heating coil.

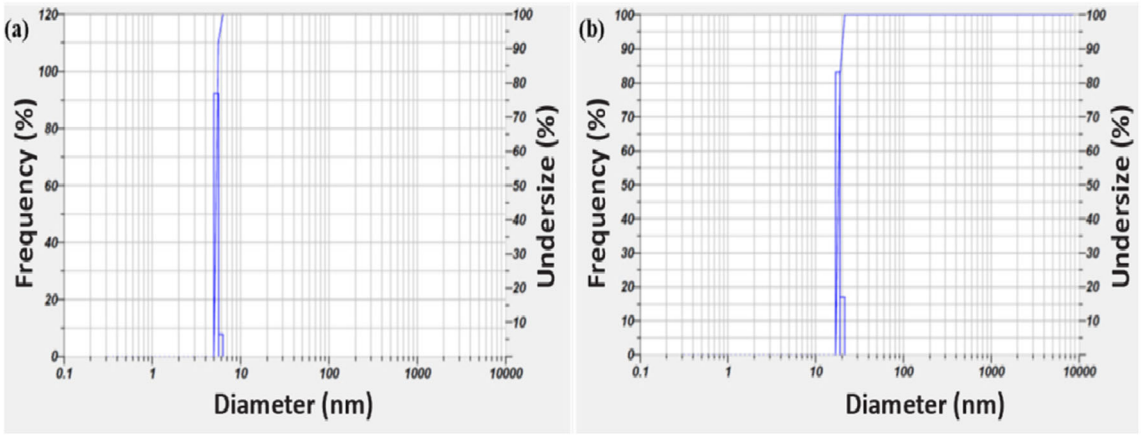

Fig. 2 Particle size distribution of (a) NS and (b) SIPX-NS

2.3.7 Cure Characteristics

RPA 2000 model Rubber Process Analyser from Alpha Technologies, USA kept at an angle of 0.5 degree and 100 cpm frequency was used for rheological characterization according to ASTM D 5289.

2.3.8 Tensile and Tear Test

Universal Testing Machine from Instron, USA was used to analyze the stress-strain properties of samples as per ASTM D 412. Test specimen un-nicked at 90° angle was used for the tear resistance test according to ASTM D 624. ASTM D 573 method was used to carry out the thermal aging analysis.

The following equation was used to determine the tensile retention percentage:

$$\text{Tensile retention}\% = \frac{\text{Tensile strengh after aging}}{\text{Tensile strength before aging}} \text{X}100 \quad (1)$$

2.3.9 Hardness and Abrasion Resistance

The shore A hardness of compression moulded samples was measured as per ASTM D 2240 using Bariess durometer. The tests were performed on unstressed samples of 6 mm thickness. A load of 12.5 N was applied and the readings were taken after 10 s of indentation when a firm contact has been established with the specimen.

The abrasion resistance of the samples was determined using Bariess DIN abrader, Germany (ASTM D 5963). The sample having a diameter of 16 ± 0.2 mm was kept on a rotating sample holder and a 10 N load was applied. Initially, a pre-run was given to the sample and its weight taken. The weight after the final run was also noted.

2.3.10 Specific Gravity and Compression Set

Specific gravity was determined as per ASTM D 297 using Densimeter at room temperature. ASTM D 395 standard aws used to measure the compression set. The samples (12.5 mm thick and 29 mm diameter) in duplicate compressed to a

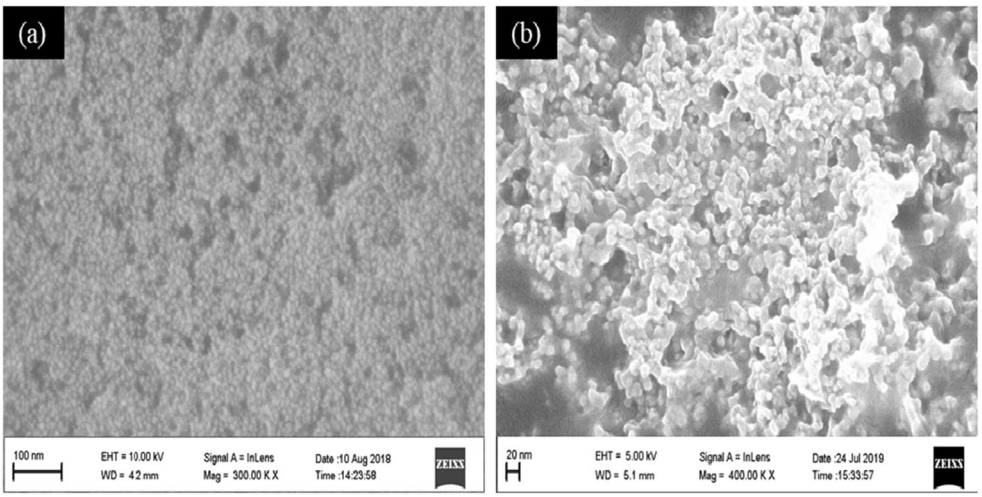

Fig. 3 Scanning electron micrographs of (a) NS and (b) SIPX-NS

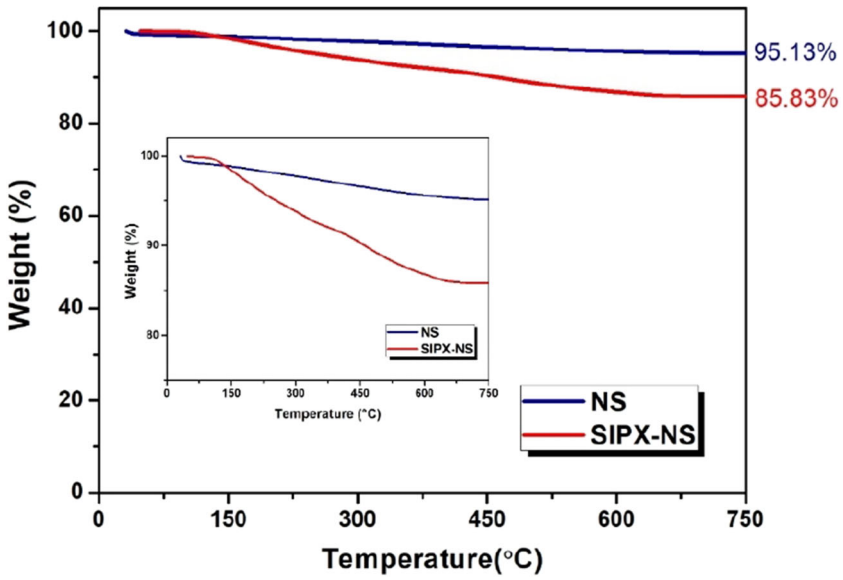

Fig. 4 TGA of NS and SIPX-NS

constant deflection (25%) were kept in an air oven at 70 °C for 22 h.

2.3.11 Heat Build-Up and Flex Crack

Heat build-up study was carried out using Dynesco Goodrich Flexometer according to ASTM D 623. The test pieces were prepared in a cylindrical shape with a diameter of 17.8 ± 0.1 mm and 25 ± 0.15 mm height by the compression moulding machine. Demattia flexing machine was used to check flex cracking and crack growth of the samples as per ASTM D 430 and ASTM D 813 respectively.

2.3.12 Rebound Resilience

Rebound resilience was measured according to ASTM D 7121 using Wallace Dunlop Tripsometer.

The following equation was used to calculate rebound resilience percentage (RB)

$$RB\% = \frac{1- \text{Cos (angle of rebound)}}{1- \text{Cos (original angle)}} X100 \quad (2)$$

Table 3 NR composites rheological data

Name of sample	ts_2 (Minutes)	t_{90} (Minutes)	M_H-M_L (dNm)
NR gum	3.04	7.31	29.39
NR 3NS	2.65	7.94	29.45
NR 3SIPX-NS	0.89	6.68	29.62
NR 4SIPX-NS	0.84	6.09	29.94
NR 5SIPX-NS	0.93	5.78	31.12

M_H - maximum torque and M_L - minimum torque

2.3.13 Crosslink Density, Swelling Index and Mol Percentage Uptake

Crosslink density, swelling index and mol percentage uptake were measured by the equilibrium swelling method.

Flory-Rehner equation was used to calculate the crosslink density of samples [25].

$$\text{Crosslink density} = \frac{1}{2M_c} \quad (3)$$

Where M_c is the molar mass of the sample between consecutive crosslinks and this can be calculated using eq. 4.

$$M_c = -\rho_r V_s V_r^{\frac{1}{3}} / \left(\ln (1-V_r) + V_r + \chi V_r^2 \right) \quad (4)$$

In eq. 4, V_s is the molar volume of solvent (for toluene,106.2 cm^3/mol); ρ_r is the rubber density (0.94 g/cm^3); V_r is the rubber volume fraction of samples at equilibrium swelling and χ is the interaction parameter between natural rubber and toluene (0.3787 from the literature [26]). Ellis and Welding equation [27] was used to calculate V_r

$$V_r = (d - f w)^{-1} / (d - f w)\rho r^{-1} + A_s \rho_s^{-1} \quad (5)$$

For all samples, eq. 6 was used to calculate the percentage solvent uptake (Qt%)

$$Qt\ mol\% = \frac{(\text{Mass of solvent sorbed/Molar mass of solvent})}{\text{Mass of polymer}} X100 \quad (6)$$

The following equation was used to determine the swelling index.

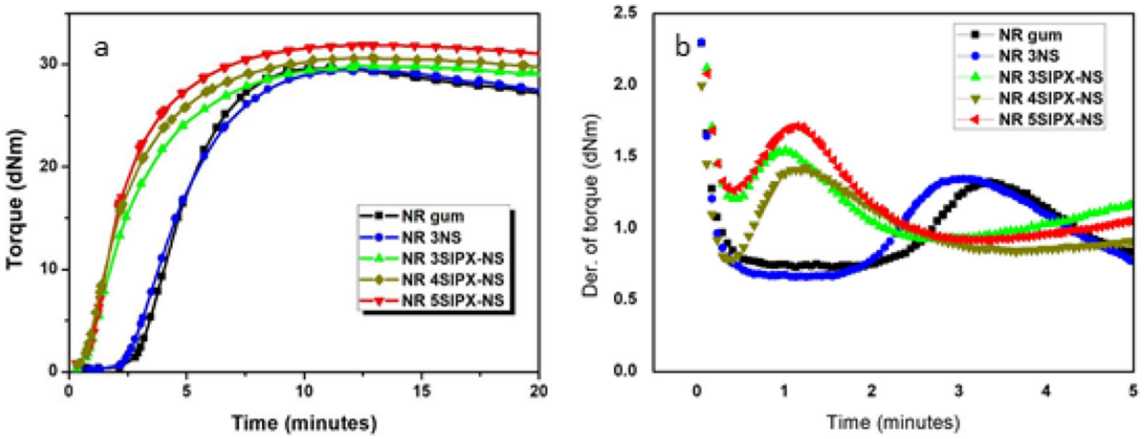

Fig. 5a Cure curve and 5b. Derivative of torque vs reaction time of NR composites

$$\text{Swelling index} = \frac{(Ws–Wi)}{Wi} X100 \quad (7)$$

Here, Ws and Wi are the swollen and initial weight of the specimen.

3 Results and Discussion

3.1 Fourier Transform Infrared Analysis

Figure 1 shows the FTIR spectra of samples NS, SIPX and SIPX-NS. In NS, the silanol hydroxyl groups stretching vibration and adsorbed moisture together constitute the peak at 3560 cm^{-1}. The peaks at 807 cm^{-1} and 1107 cm^{-1} are due to the symmetric and asymmetric stretching vibrations of Si-O-Si linkages [17]. The bending vibrations of –OH groups are responsible for a peak at 1642 cm^{-1}. In SIPX, the C=S stretching vibration leads to the absorption band at 1050 cm^{-1} and 1037 cm^{-1} [28]. The peak at 1191 cm^{-1} is due to C-O-C symmetric stretching vibration [29]. The peaks at 1377 cm^{-1} corresponds to bagging of the C-H bond in the CH_3 group of SIPX [30]. The C=S vibration peak of SIPX-NS at 1037 cm^{-1} shifts towards lower wavenumbers 1002 cm^{-1} and the peak at 1050 cm^{-1} shifts towards higher wavenumbers 1118 cm^{-1} compared with those of SIPX. The shift in these peaks is due to the coordinated structure of SIPX-NS.

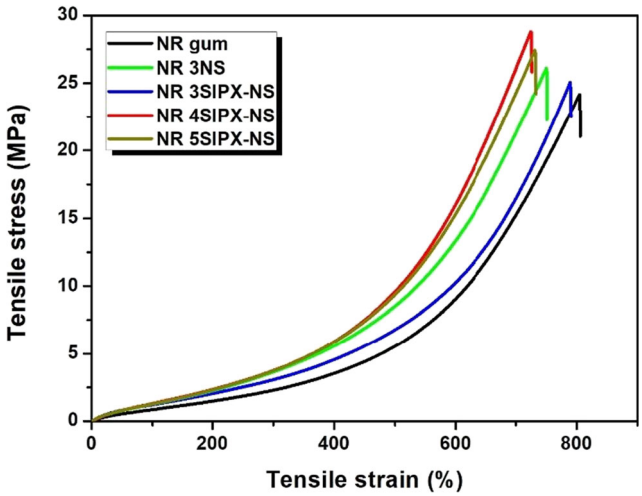

Fig. 6 Tensile stress-strain curves obtained for NR composites

3.2 Elemental Analysis

The elemental analysis of the SIPX modified nanosilica shows carbon, sulphur and sodium besides silicon and oxygen. The percentage of elements is tabulated in Table 2. The results confirm the successful modification of the silica with SIPX.

3.3 Dynamic Light Scattering Analysis (DLS)

The particle size distribution of SIPX-NS was measured using DLS. As shown in fig. 2(a), the average particle size for NS was 6 nm. The particle size of SIPX-NS was increased to 20 nm and this may be due to the modification and mild agglomeration of NS particles.

3.4 Morphological Analysis

Figure 3 shows the scanning electron micrographs of NS and SIPX-NS particles. SIPX-NS particles show morphological changes and a bigger size compared to NS. The average size of SIPX-NS measured from the micrograph was 20 nm, whereas for NS the particle size was 6 nm. This result is in agreement with the results obtained from DLS studies. Hydrogen bonding and Van der Waals forces among SIPX-NS particles lead to agglomeration also [31].

3.5 Thermogravimetric Analysis

Thermograms of NS and SIPX-NS are shown in fig. 4. Within the temperature range of 30–750 °C, two weight loss steps were exhibited by nanosilica. The release of adsorbed

Table 4 Tensile and tear properties of NR composites

Name of sample	Tensile strength (MPa)	Elongation at break (%)	Modulus at 300% elongation (MPa)	Tear strength (N/mm)
NR gum	23.35 ± 0.8	804 ± 15	2.29 ± 0.25	34.90 ± 0.9
NR 3NS	26.20 ± 0.3	751 ± 16	3.64 ± 0.13	43.62 ± 1.2
NR 3SIPX-NS	25.45 ± 0.2	790 ± 8	3.07 ± 0.28	44.71 ± 1.4
NR 4SIPX-NS	28.9 ± 0.33	726 ± 14	3.74 ± 0.03	45.94 ± 1.5
NR 5SIPX-NS	27.52 ± 0.26	732 ± 21	3.72 ± 0.07	46.05 ± 1.8

moisture is the reason for the initial weight loss on heating from 50 to 110 °C [32]. Dehydration of silanol groups occur between 400 and 600 °C results in the second stage weight loss [33]. The decomposition of modifying group in the temperature range of 150–600 °C is the reason for the major weight loss for SIPX-NS. The very low initial weight loss of SIPX-NS between 50 and 110 °C is due to the increase in hydrophobic character of silica by the presence of an organic modifying group. Analysis of percentage residue confirmed the presence of 9.3 wt% of SIPX on silica particles.

3.6 Cure Characteristics of NR Composites

Figure 5a illustrates the cure characteristics of natural rubber composites. Table 3 provides the cure parameters. The surface property, concentration and nature of filler influence the cure behavior of composites [34]. Compared to NR SIPX-NS composites, the scorch and cure time of NR gum and NR 3NS composites are higher. The increase in the cure time of NR 3NS composite may be due to the adsorption of curatives on the particles of silica. Silica particle adsorption of curatives leads to an increase in cure time for NR 3NS composite [35]. Lowering of NR SIPX-NS composite optimum cure time (t_{90}) is due to the reduction in surface hydroxyl groups of nanosilica and also the accelerating effect of SIPX present on the modified silica. The scorch time (ts_2) of modified nanosilica composites is drastically reduced due to the accelerating efficiency of SIPX. Reduction in scorch time indicates that the NR SIPX-NS composites have lower processibility. The torque values are increased with increasing SIPX-NS concentration due to the better crosslink density of composites, as indicated in Table 3.

Figure 5b shows the derivative cure curve of NR composites. It indicates the accelerating effect of modified silica on the curing reaction of NR composites. From the graph, it is clear that NR SIPX-NS composites achieved the maximum peak height quickly during the progress of reaction compared to NR gum and NR 3NS composites. The maximum peak obtained for NR gum and NR 3NS composites is at 3 min range, whereas for NR 3SIPX-NS, NR 4SIPX-NS and NR 5SIPX-NS are only at 1 min range.

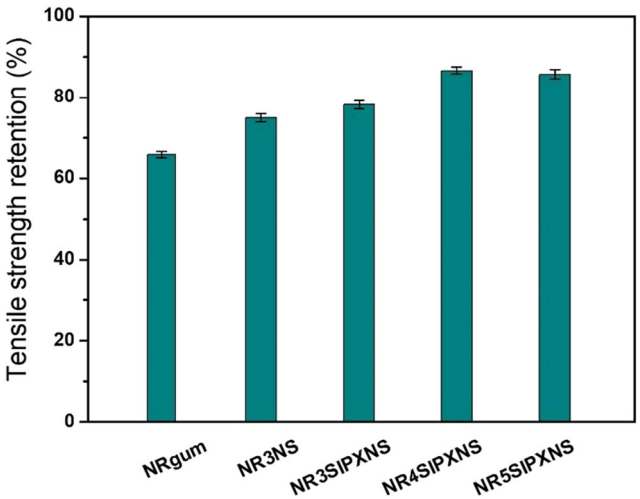

Fig. 7 Retention of tensile strength of NR composites

3.7 Stress-Strain Behaviour of NR Composites

Figure 6 shows the stress-strain behaviour obtained for all NR composites. Higher tensile strength was obtained for NR 4SIPX-NS compared to all other composites. Better rubber and filler interaction is the reason for higher tensile strength. At a higher concentration of SIPX-NS, aggregation of particles of silica causes poor interaction between the filler and the rubber [36]. In our previous work on natural rubber reinforced nanosilica composites [37], we found that the maximum tensile strength is obtained for the NR 3NS composite. In NR SIPX modified nanosilica composites NR 4SIPX-NS shows a 10% and 24% increase in tensile strength compared to NR 3NS composite and NR gum compound respectively.

Elongation at break percentage was found to be decreased with an increase in silica concentration. This is because of the restriction in the movement of polymer chains by the presence of non-deformable silica particles [38]. An increase in modified nanosilica concentration leads to an increase in tear

Table 5 Technological properties of NR composites

Sample name	Abrasion loss (cc)	Hardness (Shore A)	Dynamic compression set (%)	Heat build-up (°C)	Compression set (%)	Rebound resilience (%)
NR gum	0.32 ± 0.01	38 ± 1	2.30 ± 0.1	1 ± 0	25.6 ± 0.2	78 ± 3
NR 3NS	0.27 ± 0.02	44 ± 0.5	4.65 ± 0.1	12 ± 1	28.4 ± 0.1	68 ± 2
NR 3SIPX-NS	0.28 ± 0.05	42 ± 0.5	4.75 ± 0.2	11 ± 2	28.5 ± 0.25	68 ± 1
NR 4SIPX-NS	0.23 ± 0.01	44 ± 0.5	7.20 ± 0.2	13 ± 1	34.91 ± 0.17	65 ± 2
NR 5SIPX-NS	0.22 ± 0.01	45 ± 0.5	7.20 ± 0.3	15 ± 2	35.48 ± 0.2	63 ± 1

strength and modulus at 300% elongation. This is due to higher crosslink density and bound rubber content [11]. Elongation at break, tensile strength, modulus at 300% elongation and tear strength obtained for natural rubber composites are given in Table 4. The concentration of filler, particle size and its dispersion affect the tensile strength and modulus of the composites.

The tensile properties of the composites were studied after aging at 100 °C for 24 h, as it is very important to evaluate the performance in practical applications. The percentage retention of the tensile strength is shown in Fig. 7. NR gum shows lower retention compared to nanosilica-filled composites. Luo et al. [39] observed a similar result while studying the effect of silica and antioxidant on NR composites. NR 4SIPX-NS shows excellent tensile retention in comparison with all other natural rubber composites.

3.8 Other Technological Properties of NR Composites

Table 5 includes the tabulated values of other technological properties of NR composites. The composites showed an increase in hardness with an increase of filler loading. This is in line with the increase in modulus and crosslink density [40] of the composites.

The abrasion resistance of rubber vulcanizates depends on several factors such as filler particle size, structure, surface activity, and filler-rubber interaction [41]. The reduction in abrasion loss for NR SIPX-NS composites attributed to the improvement in service life due to the good interaction between the matrix and filler and better filler dispersion.

Table 6 Flex cracking resistance of NR composites

Sample name	Flex crack (kilocycles)	
	Initiation	Crack growth
NR 3NS	45	62
NR 3SIPX-NS	47	66
NR 4SIPX-NS	51	77
NR 5SIPX-NS	50	74

The ability of a material to recover from an applied continuous strain is measured in compression set analysis. The percentage of dynamic compression set and compression set values found to be increased with an increase in nanosilica concentration as silica is a non-resilient reinforcing filler [37]. With the increase in modulus of the composite, more restrictions in polymer chain mobility occurred even after the applied stress is removed. This is confirmed from modulus values which show a linear relationship with the compression set.

In the heat build-up test, the dissipation of energy occurs as heat because of the friction among filler particles and also between rubber matrix and filler under cyclic deformation [42]. With the increase in filler loading heat build-up of composites found to be increased. This causes a rise in fatigue failure and leads to inferior mechanical properties of the composites [43]. There is no significant change in heat build-up for NR 4SIPX-NS and NR 3NS samples as the modification improve the filler dispersion in the rubber matrix.

Table 6 shows the initial flex crack and crack growth of NR silica composites. Resistance to flex crack and crack growth is the essential dynamic properties required for the rubber products used in dynamic applications. Flex crack resistance of the NR composites mainly depends on the dispersion of filler,

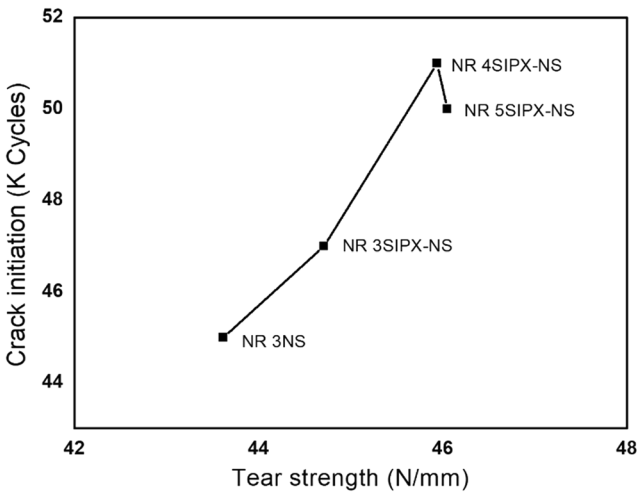

Fig. 8 Relationship between tear strength and crack initiation of NR nanocomposites

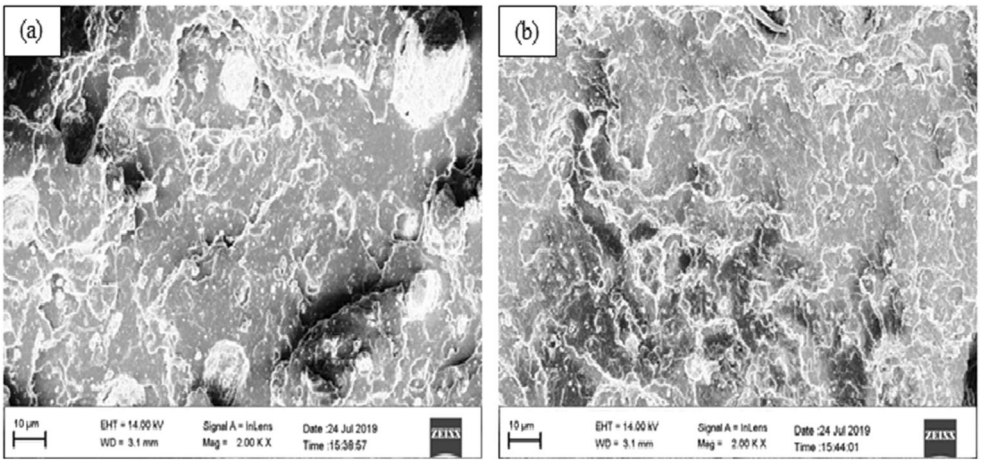

Fig. 9 FESEM images of NR 3NS and NR 4SIPX-NS composites

nature of crosslink network and concentration and mechanical oxidative aging (antidegradent present) [44, 45]. Modified nanosilica filled NR composites showed higher resistance to flex cracking and crack growth compared to unmodified nanosilica filled NR composite. This improved resistance may be due to the presence of long hydrocarbon chains in SIPX-NS, which helps better dispersion of nanosilica and improved crosslinking [46]. The lower value for both flex cracking and crack growth resistance for unmodified nanosilica NR composite was due to the agglomeration of nanosilica particles and rigid interaction of nanosilica with NR. The maximum resistance obtained for NR 4SIPX-NS composite was due to the optimum sulphur-accelerator ratio at this concentration [47].

Tear strength and fatigue life are interconnected as both are related to the breaking energy of the composite [48]. The relationship between crack initiation and tear strength is plotted in fig. 8. The plot implies that the factors which contribute to improve tear strength may be the same as the factors which contribute resistance to crack initiation. The crack initiation cycles of NR 5SIPX-NS were lower compared to NR 4SIPX-NS due to the denser crosslink formation [48], as tabulated in Table 3.

Table 7 Data from TG analysis

Name of sample	T_{on}, Onset degradation temperature (°C)	T_{max}, Maximum degradation temperature (°C)	T_{50}, Temperature at 50% degradation (°C)	Residue at 750 °C (%)
NR Gum	325	368	372	4.92
NR 3NS	328	372	375	8.57
NR 4SIP-X-NS	326	372	375	8.88

3.9 Morphology of NR Composites

The dispersion of filler in the polymer matrix determines the ultimate properties of composite samples. Stress concentration points developed inside the composites due to aggregation of particulate fillers which may lead to inferior properties while nanoparticles uniform distribution enhances the properties [11]. A little roughness and few agglomerates of silica present on NR 3NS tensile fractured surface (fig. 9(a)) indicate that the interfacial interaction between nanosilica and NR is less. NR 4SIPX-NS composite shown in fig. 9(b) is rugged with undulations and uniform filler dispersion, indicating that the matrix could transfer the applied stress to the nanosilica during the tensile test.

3.10 Thermal Stability of NR Nanosilica Composites

Figure 10 shows the thermogravimetric curves obtained for the composite samples with nanosilica, modified nanosilica and gum compound. NR gum and composites showed a single step degradation pattern. The initiation of this single step

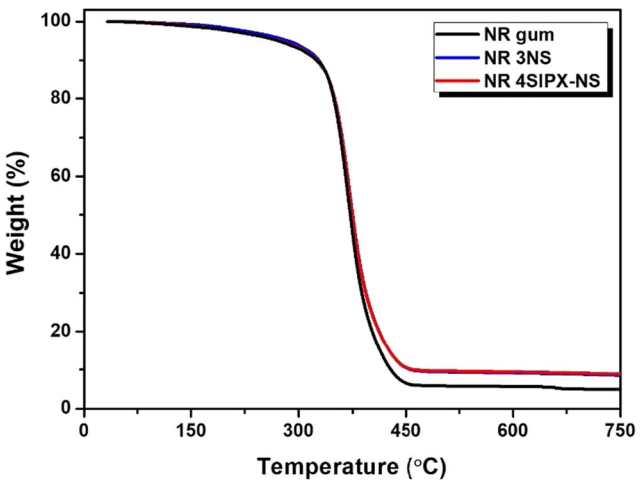

Fig. 10 TG analysis of NR 4SIPX-NS, NR 3NS and NR gum

Table 8 Thermal conductivity of NR composites

Name of sample	Thermal conductivity (Wm^{-1} k^{-1})
NR Gum	0.153
NR 3NS	0.172
NR 4SIPX-NS	0.174

degradation occurs by the thermal C-C bond chain scission followed by hydrogen transfer at the scission site [49]. NR gum showed T_{on} (degradation temperature at 10% wt. loss) at 325 °C. 3 phr nanosilica addition in NR increased T_{on} by 3 °C while 4SIPX-NS had no significant change due to the initial decomposition of SIPX on nanosilica particles. The maximum degradation temperature and temperature at 50% degradation (T_{50}) of both NR 4SIPX-NS and NR 3NS composites were same and 4 °C higher compared to gum compound. The degradation of NR depends upon the nature of metal ion present, concentration of xanthate used etc. [50]. As the amount of xanthate in SIPX-NS is low, the composite with SIPX-NS has no significant effect on thermal properties. The thermal degradation characteristics are shown in Table 7.

3.11 Thermal Conductivity of NR Composites

Thermal conductivity data for NR gum, NR 3NS and NR 4SIPX-NS composites are shown in Table 8. The thermal conductivity of polymers is influenced by the incorporation of fillers [51]. The filler nature, orientation, dispersion in the matrix, volume fraction and thermal conductivity of the filler are the major parameters contributing to thermal conductivity of composites [52]. Thermal conductivity values of NR nanosilica composites were found to be slightly higher compared to NR gum as nanosilica has a low value of thermal conductivity [53]. Minor enhancement in thermal conductivity of NR 4SIPX-NS composite compared to NR 3NS composite may be due to the better interaction, which is beneficial for the transmission of a phonon with decreased phonon scattering [54].

Table 9 Swelling index and crosslink density of NR silica composites

Sample name	Crosslink density (10^{-5} mol/g)	Swelling index (%)
NR gum	7.4 ± 0.1	356 ± 2
NR 3NS	7.93 ± 0.1	337 ± 1
NR 3SIPX-NS	8 ± 0.1	341 ± 1
NR 4SIPX-NS	8.37 ± 0.1	315 ± 2
NR 5SIPX-NS	8.40 ± 0.1	307 ± 1

3.12 Swelling Behaviour and Crosslink Density of NR Silica Composites

Rubber-filler interaction and chemical crosslinks inside the vulcanized composites definitely affect the crosslink density [55]. Solvent molecular size, mobility of polymer chains and free volume inside the composite are the main factors that affect the transport of solvent through the rubber matrix. Table 9 shows the tabulated values of swelling index and crosslink density of composites samples. NR composites showed a decrease in solvent uptake with an increase in silica concentration. Compared to the NR 4SIPX-NS composite NR 3NS sample showed higher toluene uptake. This is due to better silica-rubber interactions and uniform filler dispersion in NR 4SIPX-NS composite. The transportation of solvent molecules through the NR matrix is restricted by the uniformly distributed SIPX-NS particles. After vulcanization, mobility of the NR chains is restricted by filler particles. Maximum crosslink density was observed for the NR 5SIPX-NS sample and the value was comparable with the 4SIPX-NS containing NR composite.

4 Conclusion

We have studied the synergistic effects of the accelerator sodium isopropyl xanthate and nanosilica on the thermo-oxidative aging resistance and cure characteristics of natural rubber. We have also developed a simple and highly efficient surface modification of nanosilica using sodium isopropyl xanthate. The modification was confirmed by FTIR, EDX, FESEM, DLS and TGA. Improved rheological, mechanical and aging properties were observed for the modified silica NR composites, which could be credited to the significantly improved rubber-filler interfacial interaction, higher crosslink density and dispersion. Improved interfacial interaction and dispersion of modified silica were revealed by FESEM. NR modified silica composite had high crosslinking density and hence showed high tensile strength retention and flex crack resistance. This indicates the composite has a long service life and can be used for a wide range of applications.

Acknowledgments We thank J J Murphy Research Centre, Rubber Park India (P) Ltd., Valayanchirangara for rheological characterization and mechanical property analysis and Department of Physics, Cochin University of Science and Technology for FESEM and EDX analysis.

Availability of Data and Material My research didn't generate any data or I reused existing data.

Author Contributions Dileep P.: Conceptualization, methodology, visualization, investigation and writing. Sinto Jacob: Conceptualization, writing, reviewing and editing. Julie Chandra C.S.: Data curation and

resources. Midhun Dominic C.D.: Data curation, writing and reviewing. Poornima M.P.: Data curation, resources and reviewing. John P. Rappai: Writing, reviewing and editing. Sunil K. Narayanankutty.: Supervision, writing, reviewing and editing.

Declarations This article does not contain any studies involving animals or human participants performed by any of the authors.

Consent to Participate Not Applicable.

Consent for Publication Not Applicable.

Conflict of Interest The authors have no conflicts of interest to declare that are relevant to the content of this article.

References

1. Hu D, Jia Z, Zhong B, Chen Y, Luo Y, Jia D (2016) A facile and green preparation of nanosilica-supported antioxidant and its reinforcement and antioxidation effect on styrene-butadiene rubber. Int J Polym Anal Charact 21:185–197. https://doi.org/10.1080/1023666X.2016.1132125
2. Li Y, Han B, Liu L, Zhang F, Zhang L, Wen S, Lu Y, Yang H, Shen J (2013) Surface modification of silica by two-step method and properties of solution styrene butadiene rubber (SSBR) nanocomposites filled with modified silica. Compos Sci Technol 88:69–75. https://doi.org/10.1016/j.compscitech.2013.08.029
3. Surya I, Ismail H, Azura AR (2014) The comparison of alkanolamide and silane coupling agent on the properties of silica- filled natural rubber (SMR-L) compounds. Polym Test 40:24–32. https://doi.org/10.1016/j.polymertesting.2014.08.007
4. Ahans-Detlef Luginsland D (n.d.) Joachim Frohlich, Andre Wehmeier AG, influence of different silanes on the reinforcement of silica-filled rubber compounds. Rubber Chem Technol 75:563–580
5. Zheng J, Han D, Zhao S, Ye X, Wang Y, Wu Y, Dong D, Liu J, Wu X, Zhang L (2018) Constructing a multiple covalent Interface and isolating a dispersed structure in silica/rubber nanocomposites with excellent dynamic performance. ACS Appl Mater Interfaces 10:19922–19931. https://doi.org/10.1021/acsami.8b02358
6. Qiao B, Liang Y, Wang TJ, Jiang Y (2016) Surface modification to produce hydrophobic nano-silica particles using sodium dodecyl sulfate as a modifier. Appl Surf Sci 364:103–109. https://doi.org/10.1016/j.apsusc.2015.12.116
7. Lei H, Huang G, Weng G (2013) Synthesis of a new nanosilica-based antioxidant and its influence on the anti-oxidation performance of natural rubber. J Macromol Sci Part B Phys 52:84–94. https://doi.org/10.1080/00222348.2012.695560
8. Sondi I, Fedynyshyn TH, Sinta R, Matijević E (2000) Encapsulation of nanosized silica by in situ polymerization of tert-butyl acrylate monomer. Langmuir. 16:9031–9034. https://doi.org/10.1021/la000618m
9. Espiard P, Guyot A, Perez J, Vigier G, David L (1995) Poly(ethyl acrylate) latexes encapsulating nanoparticles of silica: 3. Morphology and mechanical properties of reinforced films. Polymer (Guildf) 36:4397–4403. https://doi.org/10.1016/0032-3861(95)96845-Y
10. Vilmin F, Bottero I, Travert A, Malicki N, Gaboriaud F, Trivella A, Thibault-Starzyk F (2014) Reactivity of bis[3-(triethoxysilyl)propyl] tetrasulfide (TESPT) silane coupling agent over hydrated silica: operando IR spectroscopy and chemometrics study. J Phys Chem C 118:4056–4071. https://doi.org/10.1021/jp408600h
11. Zhang H, Gao Y, Li F, Zhang Z, Liu Y, Zhao G (2016) Influence of silane coupling agents on vulcanised natural rubber: dynamic properties and heat buildup. Plast Rubber Compos 45:9–15. https://doi.org/10.1080/14658011.2015.1112518
12. Chen L, Jia Z, Tang Y, Wu L, Luo Y, Jia D (2017) Novel functional silica nanoparticles for rubber vulcanization and reinforcement. Compos Sci Technol 144:11–17. https://doi.org/10.1016/j.compscitech.2016.11.005
13. Zhong B, Jia Z, Hu D, Luo Y, Jia D, Liu F (2017) Enhancing interfacial interaction and mechanical properties of styrene-butadiene rubber composites via silica-supported vulcanization accelerator. Compos. Part A Appl. Sci. Manuf. 96:129–136. https://doi.org/10.1016/j.compositesa.2017.02.016
14. Mathew G, Huh MY, Rhee JM, Lee MH, Nah C (2004) Improvement of properties of silica-filled styrene-butadiene rubber composites through plasma surface modification of silica. Polym Adv Technol 15:400–408. https://doi.org/10.1002/pat.482
15. Wang X, Wang P, Jiang Y, Su Q, Zheng J (2014) Facile surface modification of silica nanoparticles with a combination of noncovalent and covalent methods for composites application. Compos Sci Technol 104:1–8. https://doi.org/10.1016/j.compscitech.2014.08.027
16. Weng P, Tang Z, Huang J, Wu S, Guo B (2019) Promoted dispersion of silica and interfacial strength in rubber/silica composites by grafting with oniums. J Appl Polym Sci 48243:48243. https://doi.org/10.1002/app.48243
17. Liu J, Cheng Y, Xu K, An L, Su Y, Li X, Zhang Z (2018) Effect of nano-silica filler on microstructure and mechanical properties of polydimethylsiloxane-based nanocomposites prepared by "inhibition-grafting" method. Compos Sci Technol 167:355–363. https://doi.org/10.1016/j.compscitech.2018.08.014
18. Guo B, Chen F, Lei Y, Chen W (2010) Significantly improved performance of rubber/silica composites by addition of sorbic acid. Polym J 42:319–326. https://doi.org/10.1038/pj.2010.4
19. Gill YQ, Saeed F, Irfan MS, Ehsan H, Shakoor A (2018) Hybrid NBR/chitosan/Nano-Silanised silica based green rubber products. J Rubber Res 21:194–208. https://doi.org/10.1007/bf03449170
20. Taylor P, Attharangsan S, Ismail H, Bakar MA, Ismail J (2014) The Effect of Rice Husk Powder on Standard Malaysian Natural Rubber Grade L (SMR L) and Epoxidized Natural Rubber (ENR 50) Composites. Polym Plast Technol Eng 51:37–41. https://doi.org/10.1080/03602559.2011.625377
21. Xu T, Jia Z, Luo Y, Jia D, Peng Z (2015) Interfacial interaction between the epoxidized natural rubber and silica in natural rubber/silica composites. Appl Surf Sci 328:306–313. https://doi.org/10.1016/j.apsusc.2014.12.029
22. Ismail H, Rusli A, Rashid AA (2005) Maleated natural rubber as a coupling agent for paper sludge filled natural rubber composites. Polym Test 24:856–862. https://doi.org/10.1016/j.polymertesting.2005.06.011
23. Gelling I (1991) Epoxidised natural rubber. Prog Rubber Plast Technol 7:271–297
24. Dileep P, Narayanankutty SK (2020) A novel method for preparation of nanosilica from bamboo leaves and its green modi fi cation as a multi-functional additive in styrene butadiene rubber. Mater Today Commun 24:100957. https://doi.org/10.1016/j.mtcomm.2020.100957
25. Flory PJ, John Rehner J (1943) Statistical Mechanics of Cross-Linked Polymer Networks I. Rubberlike Elasticity, J. Chem. Phys 11:512–520. https://doi.org/10.1063/1.1723791
26. Boonkerd K, Chuayjuljit S, Abdulraman D, Jaranrangsup W (2012) Silica-rich filler for the reinforcement in natural rubber. Rubber Chem Technol 85:1–13. https://doi.org/10.5254/1.3672114

27. Ellis B, Welding GN (1964) Estimation, from Swelling, of the Structural Contribution of Chemical Reactions to the Vulcanization of Natural Rubber. Part II. Estimation of Equilibrium Degree of Swelling, Rubber Chem. Technol 37:563–570. https://doi.org/10.5254/1.3540348
28. Wang X-H (1996) Interfacial Electrochemistry of Pyrite Oxidation and Flotation. J. Colloid Interface Sci 178:628–637. https://doi.org/10.1006/jcis.1996.0160
29. Peng H, Wu D, Abdalla M, Luo W, Jiao W, Bie X (2017) Study of the effect of sodium sulfide as a selective depressor in the separation of chalcopyrite and molybdenite. Minerals 7. https://doi.org/10.3390/min7040051
30. Shiny P, Rani DPVJ (2010) Use of sodium and potassium butyl xanthate as accelerator for room temperature prevulcanization of natural rubber latex. J. Appl. Polym. Sci 116:2658–2667. https://doi.org/10.1002/app.34057
31. Zhou C, Xu S, Pi P, Cheng J, Wang L, Yang J, Wen X (2018) Polyacrylate/silica nanoparticles hybrid emulsion coating with high silica content for high hardness and dry-wear-resistant. Prog Org Coatings 121:30–37. https://doi.org/10.1016/j.porgcoat.2018.04.001
32. Zhang C, Tang Z, Guo B, Zhang L (2019) Concurrently improved dispersion and interfacial interaction in rubber/nanosilica composites via efficient hydrosilane functionalization. Compos Sci Technol 169:217–223. https://doi.org/10.1016/j.compscitech.2018.11.016
33. Charmas B, Kucio K, Sydorchuk V, Khalameida S, Zięzio M, Nowicka A (2018) Characterization of multimodal Silicas using TG/DTG/DTA, Q-TG, and DSC methods. Colloids and Interfaces 3:6. https://doi.org/10.3390/colloids3010006
34. Zhang C, Tang Z, Guo B, Zhang L (2018) Significantly improved rubber-silica interface via subtly controlling surface chemistry of silica. Compos Sci Technol 156:70–77. https://doi.org/10.1016/J.compscitech.2017.12.020
35. Ryu C, Kim SJ, Il Kim D, Kaang S, Seo G (2016) The effect of surface area of Silicas on their reinforcing performance to styrene-butadiene rubber compounds. Elastomers Compos 51:128–137. https://doi.org/10.7473/EC.2016.51.2.128
36. Mahir N, Ismail H, Othman N (2016) Tensile, swelling and thermal aging properties of mangosteen (garcinia mangostana) peel powder filled natural rubber compounds. J Polym Mater 33:233–243
37. Dileep P, Narayanankutty SK (2020) Styrenated phenol modified nanosilica for improved thermo-oxidative and mechanical properties of natural rubber. Polym Test 82:106302. https://doi.org/10.1016/j.polymertesting.2019.106302
38. Ahmed K (2015) Hybrid composites prepared from industrial waste: mechanical and swelling behavior. J Adv Res 6:225–232. https://doi.org/10.1016/j.jare.2013.12.002
39. Luo K, You G, Zhao X, Lu L, Wang W, Wu S (2019) Synergistic effects of antioxidant and silica on enhancing thermo-oxidative resistance of natural rubber: insights from experiments and molecular simulations. Mater Des 181:107944. https://doi.org/10.1016/j.matdes.2019.107944
40. Rattanasom N, Saowapark T, Deeprasertkul C (2007) Reinforcement of natural rubber with silica/carbon black hybrid filler. Polym Test 26:369–377. https://doi.org/10.1016/j.polymertesting.2006.12.003
41. Sattayanurak S, Noordermeer JWM, Sahakaro K, Kaewsakul W, Dierkes WK, Blume A (2019) Silica-reinforced natural rubber: synergistic effects by addition of small amounts of secondary fillers to silica-reinforced natural rubber Tire tread compounds. Adv Mater Sci Eng 2019:1–8. https://doi.org/10.1155/2019/5891051
42. Yu P, He H, Jia Y, Shenghui T, Jian C, Jia D, Luo Y (2016) A comprehensive study on lignin as a green alternative of silica in natural rubber composites. Polym Test 54:176–185. https://doi.org/10.1016/j.polymertesting.2016.07.014
43. Xing W, Tang M, Wu J, Huang G, Li H, Lei Z, Fu X, Li H (2014) Multifunctional properties of graphene/rubber nanocomposites fabricated by a modified latex compounding method. Compos Sci Technol 99:67–74. https://doi.org/10.1016/j.compscitech.2014.05.011
44. Walia M, Goyal S, Kapoor KK, Suneja S, Dev S (2004) Factors that affect the fatigue life of rubber: a literature survey. J Rubber Chem Technol 77:391–412
45. Yu P, He H, Jia Y, Tian S, Chen J, Jia D, Luo Y (2016) A comprehensive study on lignin as a green alternative of silica in natural rubber composites. Polym Test 54:176–185. https://doi.org/10.1016/j.polymertesting.2016.07.014
46. Sulekha PB, Joseph R, Madhusoodanan KN, Thomas KT (2002) New oligomer-bound antioxidants for improved flex crack resistance and ozone resistance. Polym Degrad Stab 77:403–416. https://doi.org/10.1016/S0141-3910(02)00090-3
47. Cox WL, Parks CR (1966) Effect of curing systems on fatigue of natural rubber vulcanizates. Am. Chem. Soc.:785–797. https://doi.org/10.5254/1.3544883
48. J.E. Mark, B. Erman, M. Roland, The Science and Technology of Rubber, 4th ed., Academic Press, 2013. https://books.google.co.in/books?id=otzx0FCPyPcC
49. Chen Y, Peng Z, Kong LX, Huang MF, Li PW (2008) Natural rubber nanocomposite reinforced with nano silica. Polym Eng Sci 48:1674–1677. https://doi.org/10.1002/pen.20997
50. Chandra R (1981) Controlled thermal degradation of natural rubber in dilute solutions in the Presence & Absence of some metal Isopropylxanthates. Indian J Chem 20:1178–1181
51. Tsekmes A, Kochetov R, Morshuis P, Smit JJ, Iizuka T, Tatsumi K, Tanaka T (2014). How different fillers affect the thermal conductivity of epoxy composites. https://doi.org/10.1109/CEIDP.2014.6995843
52. Huang C, Qian X, Yang R (2018) Thermal conductivity of polymers and polymer nanocomposites. Mater Sci Eng R Reports 132:1–22. https://doi.org/10.1016/j.mser.2018.06.002
53. Chari VD, Sharma DVSGK, Prasad PSR, Murthy SR (2013) Dependence of thermal conductivity in micro to nano silica. Bull. Mater. Sci 36:517–520. https://doi.org/10.1007/s12034-013-0519-3
54. Yang D, Kong X, Ni Y, Gao D, Yang B, Zhu Y, Zhang L (2019) Novel nitrile-butadiene rubber composites with enhanced thermal conductivity and high dielectric constant. Compos Part A Appl Sci Manuf 124:105447. https://doi.org/10.1016/j.compositesa.2019.05.015
55. Lee J-Y, Park N, Lim S, Ahn B, Kim W, Moon H, Paik H, Kim W (2017) Influence of the silanes on the crosslink density and crosslink structure of silica-filled solution styrene butadiene rubber compounds. Compos Interfaces 24:711–727. https://doi.org/10.1080/09276440.2017.1267524